Effects of elevated CO_2 on phytoplankton community biomass and species composition during a spring *Phaeocystis* spp. bloom in the western English Channel

Matthew Keys[1, 2], Gavin Tilstone[1*], Helen Findlay[1], Claire E. Widdicombe[1], Tracy Lawson[2].

[1] Plymouth Marine Laboratory, Plymouth, UK.

[2] University of Essex, Colchester, UK.

*Corresponding author: GHTI@pml.ac.uk

Running head: Effects of elevated CO_2 during a spring *Phaeocystis* bloom at coastal station L4 in the western English Channel.

Abstract

A 21-year time series of phytoplankton community structure was analysed in relation to *Phaeocystis* spp. to elucidate its contribution to the annual carbon budget at station L4 in the western English Channel (WEC).

Between 1993-2014 *Phaeocystis* spp. contributed ~4.6% of the annual phytoplankton carbon budget at station L4. During the March – May spring bloom period, the mean *Phaeocystis* spp. biomass constituted 17% with a maximal contribution of 47% in 2001. Upper maximal weekly values above the time series mean ranged from 63 – 82% of the total phytoplankton carbon (~42 – 137 mg carbon (C) m^3) with significant inter-annual variability in *Phaeocystis* spp.. Maximal biomass usually occurred by the end of April, although in some cases as early as mid-April (2007) and as late as late May (2013).

The effects of elevated pCO_2 on the *Phaeocystis* spp. spring bloom were investigated during a fifteen-day semi-continuous microcosm experiment. The phytoplankton community biomass was estimated at ~160 mg carbon C m^3 and was dominated by nanophytoplankton (40%, excluding *Phaeocystis* spp.), *Phaeocystis* spp. (30%) and cryptophytes (12%). The smaller fraction of the community comprised picophytoplankton (9%), coccolithophores (3%), *Synechococcus* (3%), dinoflagellates (1.5%), ciliates (1%) and diatoms (0.5%). Over the experimental period, total biomass increased significantly by 90% to ~305 mg C m^3 in the high CO_2 treatment while the ambient pCO_2 control showed no net gains. *Phaeocystis* spp. exhibited the greatest response to the high CO_2 treatment, increasing by 330%, from ~50 mg C m^3 to over 200 mg C m^3 and contributing ~70% of the total biomass.

Taken together, the results of our microcosm experiment and analysis of the time series suggest that a future high CO_2 scenario may favour dominance of *Phaeocystis* spp. during the spring bloom. This has significant implications for the formation of hypoxic zones and the alteration of food web structure including inhibitory feeding effects and lowered fecundity in many copepod species.

KEY WORDS: Ocean acidification, *Phaeocystis* spp., natural phytoplankton populations, western English Channel.

1. Introduction

While coastal zones account for just 7% of the global ocean surface, their role in the global carbon cycle is crucial (Wollast, 1998). Supporting an estimated 10-15% of global ocean net annual primary production, coastal regions are responsible for more than 40% of oceanic carbon sequestration (Muller-Karger, 2005). Atmospheric CO_2 concentration has increased by around 33% over pre-industrial levels, with an on-going annual increase of ~0.4% (Wolf-Gladrow et al. 1999, Raven et al. 2005, Alley et al. 2007). The dissolution of this excess CO_2 into the surface ocean directly affects the carbonate system which has lowered pH by ~0.1 units, from 8.21 to 8.10 over the last ~250 years. Further decreases are predicted by 0.3-0.4 pH units by the end of this century (Doney et al., 2009; Orr et al., 2005), a phenomenon commonly referred to as ocean acidification (OA). The physiological and ecological aspects of the phytoplankton response to this changing environmental factor holds the potential to alter phytoplankton community composition, community biomass and to feedback to biogeochemical cycles (Boyd and Doney, 2002).

Marine phytoplankton have been shown to exhibit sensitivity to elevated partial pressure of CO_2 in seawater (pCO_2) in growth and photosynthetic rates, in both laboratory studies using model species in culture and on natural populations in the field (e.g. Endo et al., 2013; Eggers et al., 2013; Feng et al., 2009; Hare et al., 2007; Schulz et al., 2008; Tortell et al., 2002). Since a wide variety of processes are affected, high variability in responses has been reported across and within taxa. For example, the response of diatoms under elevated pCO_2 is not straight forward. Diatom dominated natural communities exhibited no increase in growth under pCO_2 elevated to 800 µatm during shipboard incubations (Tortell et al., 2000). The diatom *Skeletonema costatum* also showed no increase in growth during laboratory studies at 800 µatm

pCO_2 (Burkhardt and Riebesell, 1997), but increased growth rates at 750 µatm pCO_2 during a mesocosm experiment (Kim et al., 2006). Feng et al., (2010) observed dominance of the large centric *Chaetoceros* spp. relative to the smaller pennate *Cylindrotheca closterium* regardless of other experimental factors during shipboard incubations under pCO_2 elevated to 760 ppm. Conversely, Coello-Camba et al., (2014) observed significant increases in growth of smaller centric diatoms (≤ 7 µm) and a decline in growth rates of larger centric diatoms (≥ 11 µm) under pCO_2 elevated to 1000 ppm during bottle incubations of an arctic phytoplankton community. Coccolithophores exhibit no change in growth rates but increased particulate organic carbon content and decreased inorganic carbon content (calcification) (Barcelos e Ramos et al., 2010; Feng et al., 2008) , whereas for the lesser-studied *Phaeocystis* spp. a decrease or no change in growth rates have been observed (Chen and Gao, 2011; Thoisen et al., 2015). The few studies on natural populations suggest that elevated pCO_2 may lead to a shift in community composition with consequences for overall rates of primary production through the pCO_2 influence on photosynthesis, elemental composition and calcification of marine phytoplankton (Riebesell, 2004).

Phaeocystis spp. are ubiquitous with a unique polymorphic life-cycle, alternating free-living solitary (~6µm in size) and colonial (~2mm in diameter) cells, a process that changes organism bio-volume by 6 to 9 orders of magnitude (Verity et al., 2007). As such *Phaeocystis* spp. can outcompete other phytoplankton and form massive blooms (up to 10 mg C m^{-3}) with impacts on food webs, global biogeochemical cycles and climate regulation (Schoemann et al., 2005). Since *Phaeocystis* spp. produce dimethylsulfoniopropionate (DMSP) their blooms also provide an important source of dimethylsulphide (DMS) (Stefels et al., 1995) playing a key role in the transfer of carbon and sulphur between ocean and atmosphere and vice versa (Liss *et al.*, 1994). While not a highly toxic algal species, *Phaeocystis* spp. are considered a harmful algal species (HAB) when biomass reaches sufficient concentrations to cause anoxia and mucus foam which can clog the feeding apparatus of zooplankton and fish (Eilertsen & Raa, 1995). Along the European coasts of the North Sea dense blooms of *Phaeocystis globosa* known to impact

ecosystem function have been well documented as localised events for many years (Lancelot and Mathot, 1987). More recently, other continents with nutrient enriched waters have reported massive blooms such as the Arabian Gulf and southeast coastal waters of China (Lancelot et al., 2002; Schoemann et al., 2005). In these ecosystems, *P. globosa* bloom formation is predominantly a result of anthropogenic factors, i.e. nutrient inputs via riverine and land run-off routes (Cadée and Hegeman, 2002). Consequently, *Phaeocystis* spp. have been identified as key water disturbance indicator species (Tett et al., 2007) and recommendations for decreasing its abundance to that of non-problem areas and good ecological status have been made in the scope of the OSPAR strategy (Ospar, 2005) and the Water Framework Directive of the European Union (2000/60/EC) (Lancelot et al., 2009). Dense blooms of *Phaeocystis antarctica* colonies are also observed in naturally nutrient rich waters, however, such as the Ross Sea (DiTullio et al., 2000), Greenland Sea and Barents Sea (Eilertsen et al., 1989; Wassmann et al., 1990). Given the ecological, global biogeochemical and climate regulation relevance, *Phaeocystis* spp. are a highly suitable and a significant model phytoplankton species to study in the context of OA.

Phytoplankton species composition, abundance and biomass has been measured at the time-series station L4 in the western English Channel (WEC) since 1992, to evaluate how global changes could drive future shifts in phytoplankton community structure and carbon biogeochemistry. The goals of the present study were to investigate: 1) the effects of elevated pCO_2 on phytoplankton community structure and the relative species contribution to community biomass during the spring bloom succession to *Phaeocystis* spp. and 2) assess the natural variability in phytoplankton community structure and the carbon biomass of *Phaeocystis* spp. at station L4 over two decades (1993-2014). We hypothesized that community biomass will increase under a high CO_2 regime and that succession to *Phaeocystis* spp. may be reduced in magnitude.

2. Materials and Methods

2.1. Time series – Phytoplankton community composition

Station L4 (50° 15'N, 4° 13'W) is located 13km SSW of Plymouth in a water depth of ~54m (Harris, 2010) and is regarded as one of Europe's principal coastal time series sites. Sampling is conducted on a weekly basis (weather permitting) and has been on-going since 1988 (http://www.westernchannelobservatory.org). Phytoplankton taxonomic composition was enumerated from seawater samples collected from 10m depth, fixed with 2% (final concentration) Lugol's iodine solution and analysed by inverted light microscopy using the Utermöhl counting technique (Utermöhl, 1958; Widdicombe *et al.*, 2010). For phytoplankton carbon biomass values; taxa-specific mean cell bio-volumes were calculated following Kovala & Larrance, (1966) and converted to carbon using the equations of Menden-Deuer & Lessard, (2000). Additionally, samples for the current study were taken from 10 m depth for the analysis of the macro-nutrients; nitrite, nitrate, silicate, phosphate and ammonium and analysed using the methods described by Woodward & Rees, (2001).

2.2. Elevated pCO_2 perturbation experiment

Experimental seawater containing a natural phytoplankton community was sampled at station L4 (50° 15'N, 4° 13'W) (**Fig 1.**) on 13th April 2015 via a high volume, wide aperture trace-metal clean manual diaphragm pump system from 10 m depth (40 L volume). The experimental seawater was pre-filtered through a 200 µm Nitex mesh to remove zooplankton grazers, into two 20 L acid-cleaned carboys. In addition, 320 L of seawater was collected into sixteen 20 L acid-cleaned carboys from the same depth for use as experimental media. Immediately upon return to the laboratory the media seawater was filtered through an in-line 0.2 and 0.1 µm filter (Acropak™, Pall Life Sciences) then stored in the dark at 11°C until use. The experimental seawater was gently and thoroughly mixed and transferred in equal parts from each carboy (to ensure homogeneity) to sixteen 2.5 L borosilicate incubation bottles (2 sets of 8 replicates). The remaining experimental seawater was sampled for initial (T0) concentrations of nutrients, chlorophyll *a*, total alkalinity and dissolved inorganic carbon and was also used to characterise

the starting experimental phytoplankton community. A semi-continuous closed incubation culture system linked the replicate incubation bottles to two 22 L media reservoirs filled with the filtered seawater media which was aerated with CO_2 free air and 5% CO_2 in air, precisely mixed using a mass flow controller (Bronkhorst UK Limited). This CO_2 enriched seawater media was then used for the microcosm dilutions, adjusted as per the following treatments: 1) Ambient pCO_2 (control at ~340 µatm, matching station L4 in situ values) and 2) Elevated pCO_2 (high CO_2 at ~800 µatm, predicted for the end of this century assuming the IPCC ' business as usual' scenario' (Alley et al., 2007)).

Initial nutrient concentrations (measured at 1.4 µM nitrate + nitrite and 0.05 µM phosphate on 13th April 2015) were amended to 8µM nitrate+nitrite and 0.5 µM phosphate replicating mean pre-spring bloom values at station L4. As the phytoplankton community was in the transitional phase from diatoms to nanophytoplankton, the in situ silicate concentration was maintained to reproduce the silicate concentrations typical of this time of year (Smyth et al., 2010). Media transfer and sample acquisition was facilitated by peristaltic pumps and daily dilution rates were set between 10-13% of the incubation bottle volume following 24 hrs acclimation. Thus, CO_2 enriched seawater was added to the high CO_2 treatment replicates every 24 hrs, acclimating the natural phytoplankton population to increments of elevated pCO_2 from ambient to ~800 µatm over 8 days followed by maintenance at ~800 µatm as per the method described by Schulz *et al*,(2009). This protocol was preferred since some phytoplankton species are inhibited by the mechanical effects of direct bubbling (Riebesell et al., 2010; Shi et al., 2009) which can cause a reduction in growth rates and the formation of aggregates (Love et al., 2016).

All glassware was autoclaved and all sampling equipment, PTFE and Marprene™ tubing was rigorously washed with 10% HCl, rinsed thoroughly with milli-Q ultrapure™ water (Millipore Corporation, USA), followed by a thorough rinse with FSW. The incubation bottles were maintained at 11 °C in a flow-through seawater bath (temperature was monitored twice daily) to replicate in situ temperature on the day of sampling. Light was supplied by a cool white LED

light bank at irradiance of ~200 µmol photons m^{-2} s^{-1} on a 16 : 8 hour light : dark cycle. Incubation bottles were inverted and gently agitated twice each day to maintain phytoplankton cells in suspension and also prior to sampling to ensure homogeneity.

2.3. Analytical methods – experimental seawater

2.3.1. Chlorophyll *a*

Chlorophyll *a* (chl *a*) was measured every three days in each incubation bottle. 100 mL triplicate samples from each replicate were filtered onto 25 mm GF/F filters, extracted in 90% acetone overnight at -20 °C and chl *a* was estimated on a Turner Trilogy ™ fluorometer using the non-acidified method of Welschmeyer (1994). The fluorometer was calibrated against a stock chl *a* standard (*Anacystis nidulans*, Sigma Aldrich, UK), the concentration of which was determined with a Perkin Elmer™ spectrophotometer at wavelengths 663.89 and 750.11 nm.

2.3.2. Carbonate system

70 mL samples for total alkalinity (TA) and dissolved inorganic carbon (DIC) analysis were collected every three days from each experimental replicate, stored in amber borosilicate bottles with no head space and fixed with 40 µL of super-saturated Hg_2Cl_2 solution for later determination (Apollo SciTech™ Alkalinity Titrator AS-ALK2; LiCOR™ 7000 DIC analyser). Duplicate measurements were made for TA and triplicate measurements for DIC. Carbonate system parameter values for media and treatment samples were calculated from TA and DIC measurements using the programme CO_2sys (Pierrot et al., 2006) with dissociation constants of carbonic acid of Mehrbach *et al*., (1973) refitted by Dickson and Millero (Dickson and Millero, 1987).

2.3.3. Phytoplankton community analysis

Phytoplankton community analysis was performed by flow cytometry (Becton Dickinson Accuri ™ C6) for the 0.2 to 18 µm size fraction following Tarran *et al.*, (2006). FlowCAM™ (Fluid

Imaging Technologies™) flow-through analysis was used for the 18-100 µm size fraction following the method described by Poulton & Martin, (2010) and light microscopy was used to enumerate cells > 100 µm (BS EN 15204,2006). For flow cytometry, 2 mL samples fixed with glutaraldehyde to a final concentration of 2% were taken every five days, flash frozen in liquid nitrogen and stored at -80 °C for later analysis. For FlowCAM, 250 mL samples fixed with acid Lugol's iodine to a final concentration of 1% were also taken every five days and stored in cool, dark conditions. Concentrated aliquots were filtered through a 100 µm Nitex mesh prior to analysis to avoid larger phytoplankton cells blocking the FlowCAM flow cell. The Nitex mesh was back-washed by gently pipetting 3mL of sample media on the reverse side to remove residual large cells. This was carefully decanted into Hydro-Bios™ settling chambers prior to analysis using an Olympus™ IMT-2 inverted light microscope. All cells in the settling chambers were identified and enumerated and the calculated cell concentrations combined with the FlowCAM data.

2.3.4. Phytoplankton community biomass

The smaller size fraction identified and enumerated through flow cytometry; picophytoplankton, nanophytoplankton, *Synechoccocus*, coccolithophores and cryptophytes were converted to carbon biomass (mg C m^3) using a spherical model to calculate mean cell volume:

$$(\frac{4}{3} * \pi * r^3)$$

and a conversion factor of 0.22 pg C μm^{-3} (Booth, 1988). A conversion factor of 0.285 pg C μm^{-3} was used for coccolithophores (Tarran et al., 2006) and a cell volume of 113 μm^3 and carbon $cell^{-1}$ value of 18 pg applied for *Phaeocystis* spp. (Widdicombe *et al.*, 2010) . *Phaeocystis* spp. were identified and enumerated separately to the nanophytoplankton class due to high observed abundance. Mean cell measurements of individual species/taxa were used to calculate

227 cell bio-volume for the 18 µm + size fraction according to Kovala and Larrance (1966) and
228 converted to biomass according to the equations of Menden-Deuer & Lessard, (2000).

229

230 **2.4. Statistical analysis**

231 Weekly biomass values from the L4 time-series were averaged over years to elucidate the
232 variability and seasonal cycles of *Phaeocystis* spp. and total phytoplankton carbon biomass
233 (excluding *Phaeocystis* spp.). Trends in *Phaeocystis* spp. biomass over time were investigated
234 using linear regression performed with a Generalised Least Squares model (gls) incorporating
235 an auto-regressive correlation structure of the order (1) to account for auto correlation. A
236 generalised linear model (glm) was used to test for differences in biomass between years. In
237 order to test for effects of high CO_2 and to account for possible time dependence of the
238 measured response variables (Chl *a*, C:chl *a*, total community biomass and biomass of individual
239 species), glm models with the factors pCO_2 and time were applied to the data following target
240 pCO_2 equilibration between days (T)9 and (T)14. Where main effects were established, pairwise
241 comparisons were performed using the method of Herberich *et al.*, (2010) for data with non-
242 normality and/or heteroscedasticity. Analyses were conducted using the R statistical package (R
243 Core Team (2014). R: A language and environment for statistical computing. R Foundation for
244 Statistical Computing, Vienna, Austria).

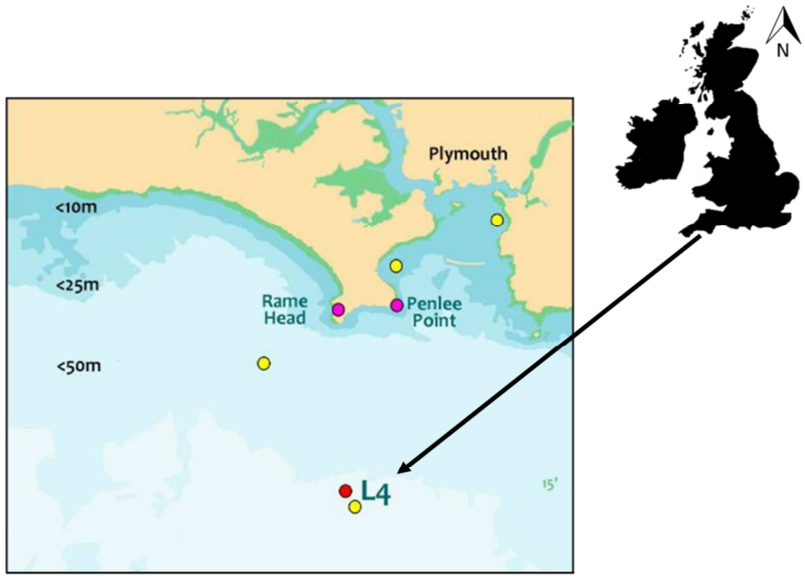

Fig 1. Location of coastal station L4, western English Channel

3. Results

3.1. Station L4 time-series, *Phaeocystis* spp. biomass in the WEC

Over the time series from 1993 to 2014, the annual mean total phytoplankton biomass sampled at L4 was 1646 (± 521 sd) mg C m^3, with annual mean *Phaeocystis* spp. biomass of 72 (± 69 sd) mg C m^3. Maximum total annual phytoplankton biomass occurred in 1997 (3206 mg C m3) and minimum values were in 2007 (998 mg C m^3) when the associated annual *Phaeocystis* spp. biomass were 121 and 75 mg C m^3 respectively (**Fig 2. A.**). *Phaeocystis* spp. contributed 4.6% of the total phytoplankton annual carbon budget, which peaked at ~16% in 2001 (~270 mg C m^3). **Fig 2. B.** shows the biomass trends over the March – May seasonal bloom period. *P. globosa* and *P. pouchetii* were both recorded at the L4 time-series site, but were grouped as *Phaeocystis* spp. due to the inherent difficulties in distinguishing single cells using microscopy.

Weekly *Phaeocystis* spp. biomass recorded from January to December throughout the time series ranged from below the limit of detection to 137 mg C m^3 (**Fig 3. A.**). Bloom initiation occurred as early as mid to late March (2007 and 2011). The bloom peak (taken as an increase

in biomass > 0.5 mg C m^3) usually occurred by the end of April, though in 2007 it was mid-April and in 2013 it was late May. The mean yearly maximal biomass peak was 41.6 (± 39.3 sd) mg C m^3 (**Fig 3. B.**). The generalised linear model highlighted significant inter-annual variability in *Phaeocystis* spp. biomass between 1993 and 2014 with biomass in 2001 significantly greater than any other year throughout the time series period, when maximal biomass reached 137 mg C m^3 ($z = 3.355$, $p < 0.001$). Half of the 21 years analysed showed a maximal peak *Phaeocystis* spp. biomass range between 42 – 137 mg C m^3 (above the time series mean maxima peak), significantly higher than all other years over the time-series ($z = -6.695$, $p < 0.0001$). Biomass as low as between 0.09 – 1.5 mg C m^3 however, was observed during the seasonal bloom in 6 out of the 21 years (**Table 3.**).

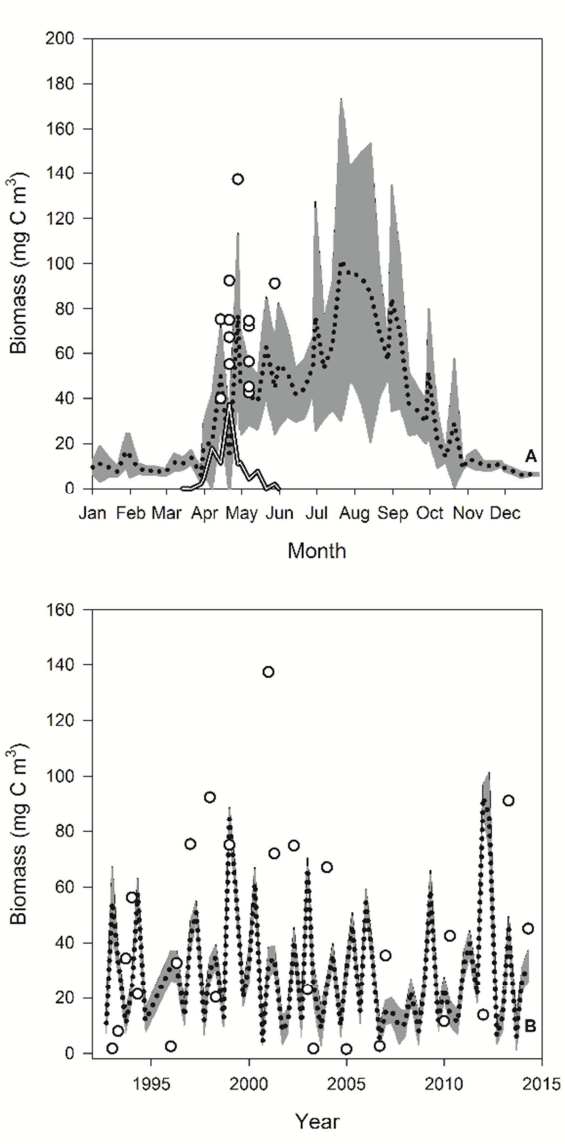

Fig 2. A. Temporal monthly profile of total phytoplankton carbon biomass at station L4 between 1993 – 2014. Dotted line is weekly mean total phytoplankton excluding *Phaeocystis* spp., grey area is standard deviation, inverse white line is mean *Phaeocystis* spp. carbon biomass and open circles are maximal weekly *Phaeocystis* spp. biomass values above the time series mean maxima value of 41.6 mg C m^3. **B**. Temporal seasonal profile of total phytoplankton carbon biomass during the spring bloom period (March – May) between 1993 – 2014. Dotted line is mean total phytoplankton excluding *Phaeocystis* spp., grey area is standard deviation and open circles are monthly maximal *Phaeocystis* spp. biomass values.

Total phytoplankton biomass peaked during the spring bloom period, typically between March and May and was highest (215 mg C m^3) when *Phaeocystis* spp. biomass increased above the time series mean peak maxima (to 56 mg C m^3). Throughout the time-series *Phaeocystis* spp. maximal biomass (above the mean maximal biomass) contributed between 26% (1994) – 82%

(1998 and 2013) of phytoplankton carbon, while total *Phaeocystis* spp. biomass over the March – May bloom period contributed a mean value of 17% to total phytoplankton carbon, between 20%-47% during years of high biomass above the mean maxima (i.e. 2001 and 2010) and between 0.1% to 13.9% during years of low biomass (i.e. 2006, 2001 and 1999). Mean bloom duration over the time-series was 22 days with a range between 6 days (2000) and 44 days (1994). Biomass showed a positive slope from 1993-2014 indicating an overall increase in *Phaeocystis* spp. carbon over the time-series, however this relationship was not significant (T = 1.86, p = 0.07).

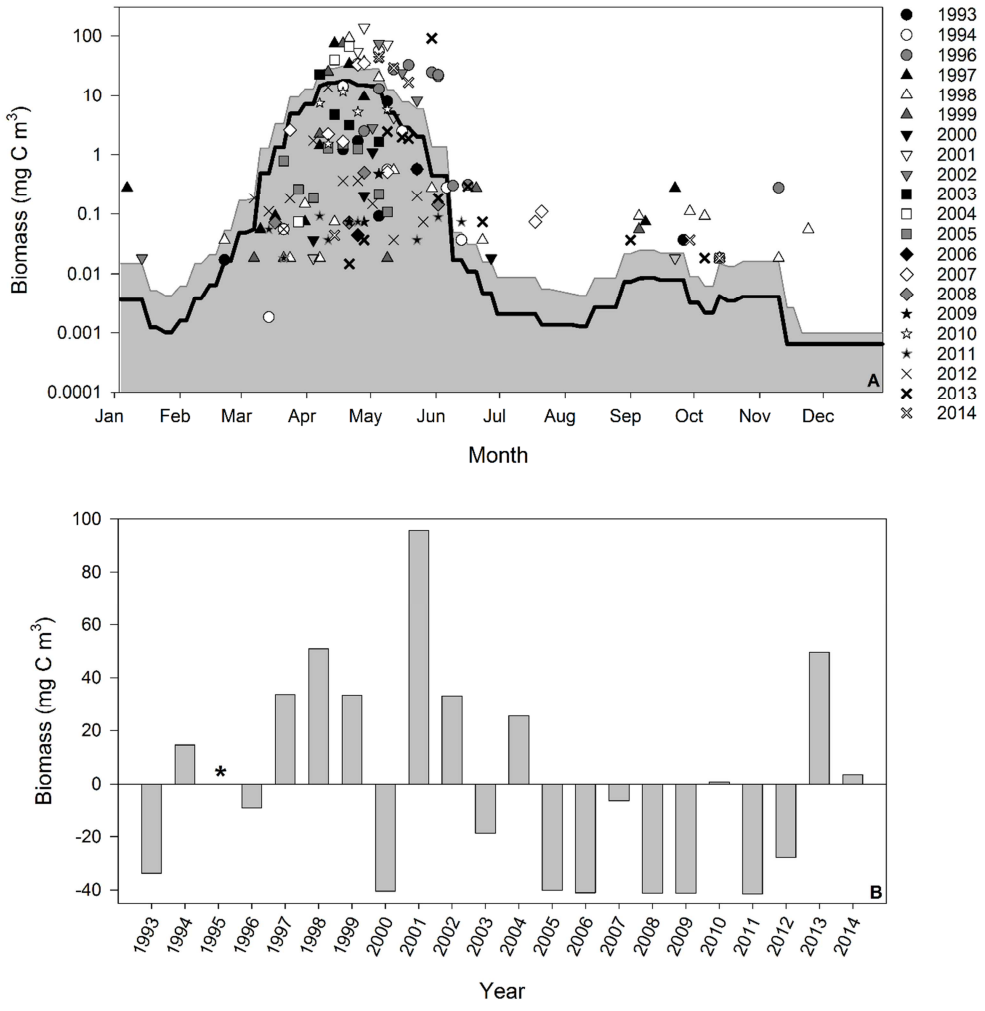

Fig 3. A. Seasonal profiles of *Phaeocystis* spp. carbon biomass (common log scale) between 1993 – 2014. Black line is smoothed running average over the time-series, grey area is the standard deviation and all symbols are observed data values by year. **B.** Annual anomalies of maximal *Phaeocystis spp.* carbon biomass above and below the time series mean maxima of 41.6 mg C m^3. * Insufficient data 1995.

3.2. Elevated pCO_2 perturbation experiment

Chl *a* concentration in the WEC and the Celtic Sea ranged between 0.4 – 6.0 mg m^3 from 8th – 14th April (**Fig 4. A.**). Declining nitrate and silicate concentrations at station L4 from February coincided with a chl *a* peak in early March, indicating the presence of an early diatom bloom. A second chl *a* peak was evident during April, indicating that our sample timing coincided with the successional phase from diatoms to the nanophytoplankton functional group / *Phaeocystis* spp. (**Fig 4. B.**). A diverse diatom community dominated by *Cocinodiscus wailesii* was observed in 200 µm net trawl samples from station L4 from late February into March and *Phaeocystis* spp. colonies were observed throughout April (data not shown).

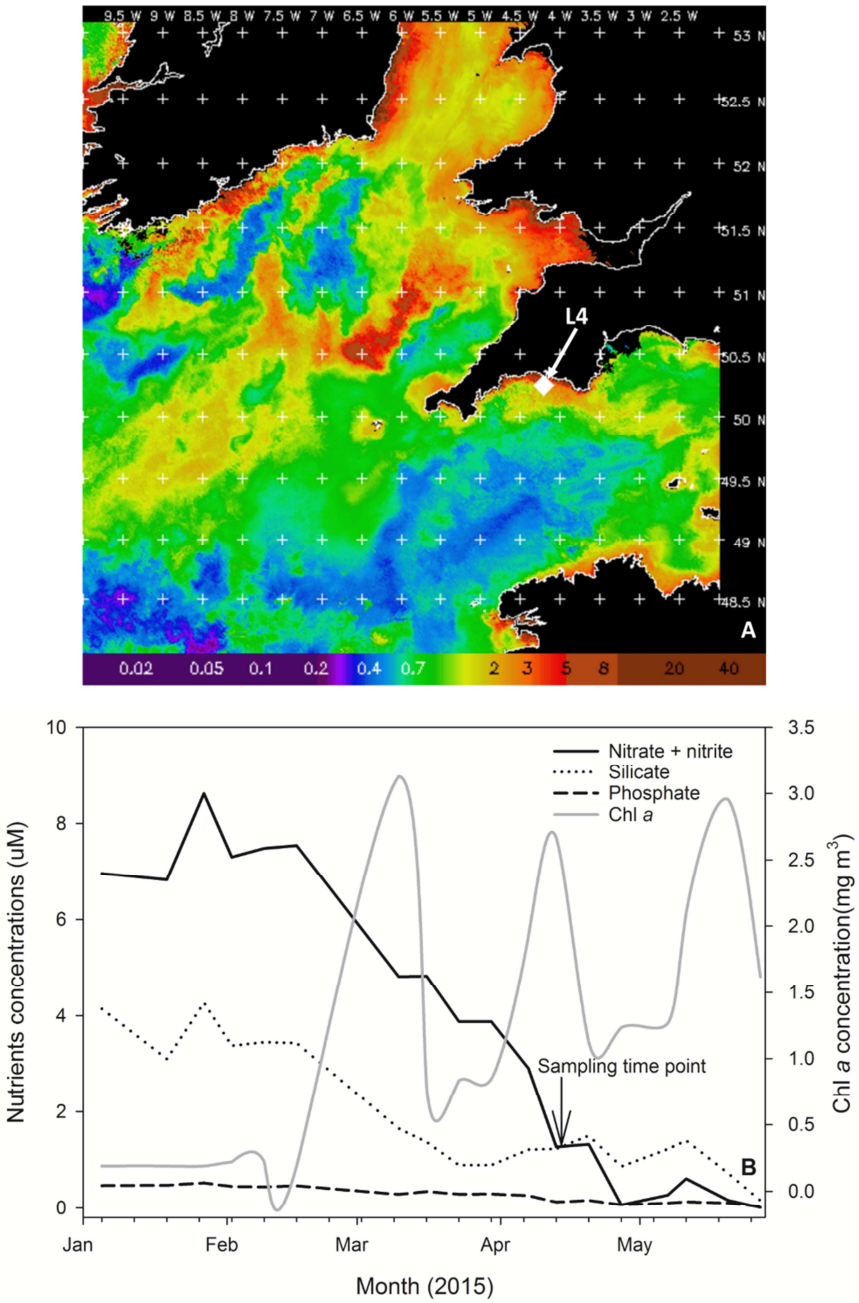

Fig 4. A. MODIS weekly composite chl *a* image of the western English Channel covering the period 8th – 14th April (coincident with the week of phytoplankton community sampling for the present study), processing courtesy of NEODAAS. The positon of coastal station L4 is marked with a white triangle. **B.** Profiles of weekly nutrient and Chl *a* measurements from station L4 at a depth of 10 m over the first half of 2015 in the months prior to experimental phytoplankton community sampling (indicated by black arrow and text).

3.2.1. Carbonate system

Mean pCO_2 values of media for the control and high CO_2 treatments were 361 (± 56 sd) and 1006 (± 61 sd) µatm respectively. Due to the dilution volume regime of the phytoplankton

community incubations, full equilibration to the target pCO_2 value (800 µatm) within the high CO_2 treatment incubations was achieved at T8. The high pCO_2 treatment incubations were slowly acclimated to rising pCO_2 over 8 days while the ambient control pCO_2 incubations were acclimated at the same ambient carbonate system values as that from station L4 on the day of sampling. Following equilibration, the mean pCO_2 values within the control and high CO_2 incubations were 350 (± 95 sd) and 812 (± 39 sd) µatm respectively (**Fig 5. A–D.**).

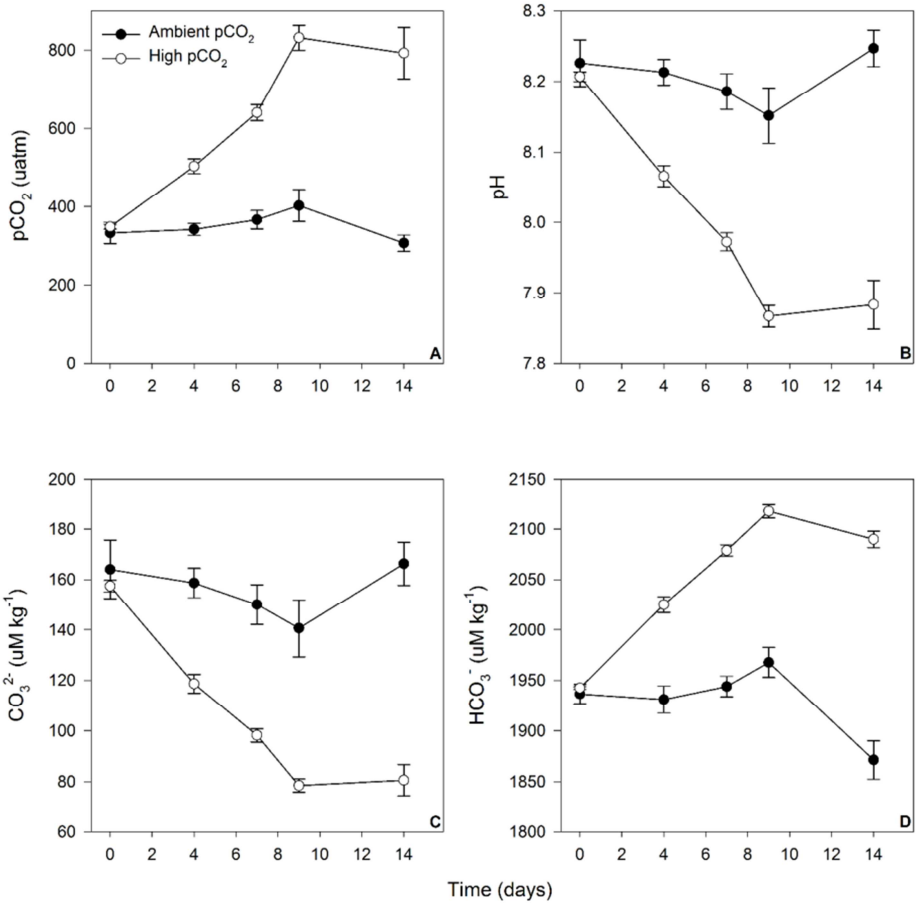

Fig 5. Carbonate system values of the experimental phytoplankton incubations. **A.** partial pressure of CO_2 in seawater (pCO_2), **B.** pH on the NBS scale, **C.** carbonate concentration (CO_3^{2-}) and **D.** bicarbonate concentration (HCO_3^-) were estimated from direct measurements of total alkalinity and dissolved inorganic carbon.

3.2.2. Chlorophyll *a*

Mean chl *a* concentration in the experimental seawater at T0 was 4.15 (± 0.38 sd) mg m^3. The concentration dropped between T0 and T6 which in the control was 1.2 (± 0.27 sd) mg m^3 at T6

337 and in the high CO_2 treatment was 1.87 (± 0.24 sd) mg m^3. Both control and high CO_2 treatments
338 showed a positive response to media dilutions from T6 onwards with no significant difference
339 in increased chl *a* concentration following target pCO_2 equilibration at T8. Final concentrations
340 were close to starting values, indicating that community net production was in balance with the
341 dilution rate. There was a significant increase in chl *a* concentration in both treatments over
342 time ($z = 2.437$, $p < 0.05$) (**Table 1.**). Mean chl *a* values on the final day of the experiment (T14)
343 were 4.1 (± 0.55 sd) and 3.5 (± 0.86 sd) mg m^3 for the control and high CO_2 treatment
344 respectively (**Fig 6. A.**).

345 ### 3.2.3. Phytoplankton biomass

346 The starting biomass was estimated at ~160 mg C m^3 in both treatment groups. The community
347 was dominated by nanophytoplankton (excluding *Phaeocystis* spp. ~40%), *Phaeocystis* spp.
348 (~30%) and cryptophytes (~12%). Picophytoplankton contributed ~9% of total biomass while
349 the remaining 10% comprised diatoms, phytoflagellates, *Synechococcus*, ciliates,
350 coccolithophores and dinoflagellates in low abundance.

351 While total community biomass in both treatments declined to T9, the biomass in the high CO_2
352 treatment increased significantly from 110 to 305 mg C m^3 between T9 and T14 ($z = 12.89$, $p <$
353 0.0001) (**Table 1., Fig 6. B.**) showing a 90% increase. The control community also increased
354 significantly between T9 and T14 and was restored to the initial starting value of 160 mg C m^3
355 showing no overall net gain over the experimental period. Pairwise comparisons between the
356 treatments showed the high CO_2 treatment total biomass to be significantly greater than the
357 control at T14 ($t = 10.787$, $p < 0.001$). In both treatments there was a significant difference in
358 C:chl *a* (mg C m^3:mg chl *a* m^3) over time ($z = 6.684$, $p <0.0001$). For the control, the ratio was
359 22.75 at T9 and 39.97 at T14, whereas for the high CO_2 treatment the ratio significantly
360 increased to 40.38 at T9 and 90.4 at T14, ($z = 6.778$, $p < 0.0001$, **Table 1., Fig 6. C.**).

Phaeocystis spp. decreased in the control community from T0 to T5 followed by a sharp increase at T9 to T14, from 17 to 91 mg C m^3. It dominated the control community, contributing 56% of overall biomass, more than any other group at T14 and increased by almost 90% compared to

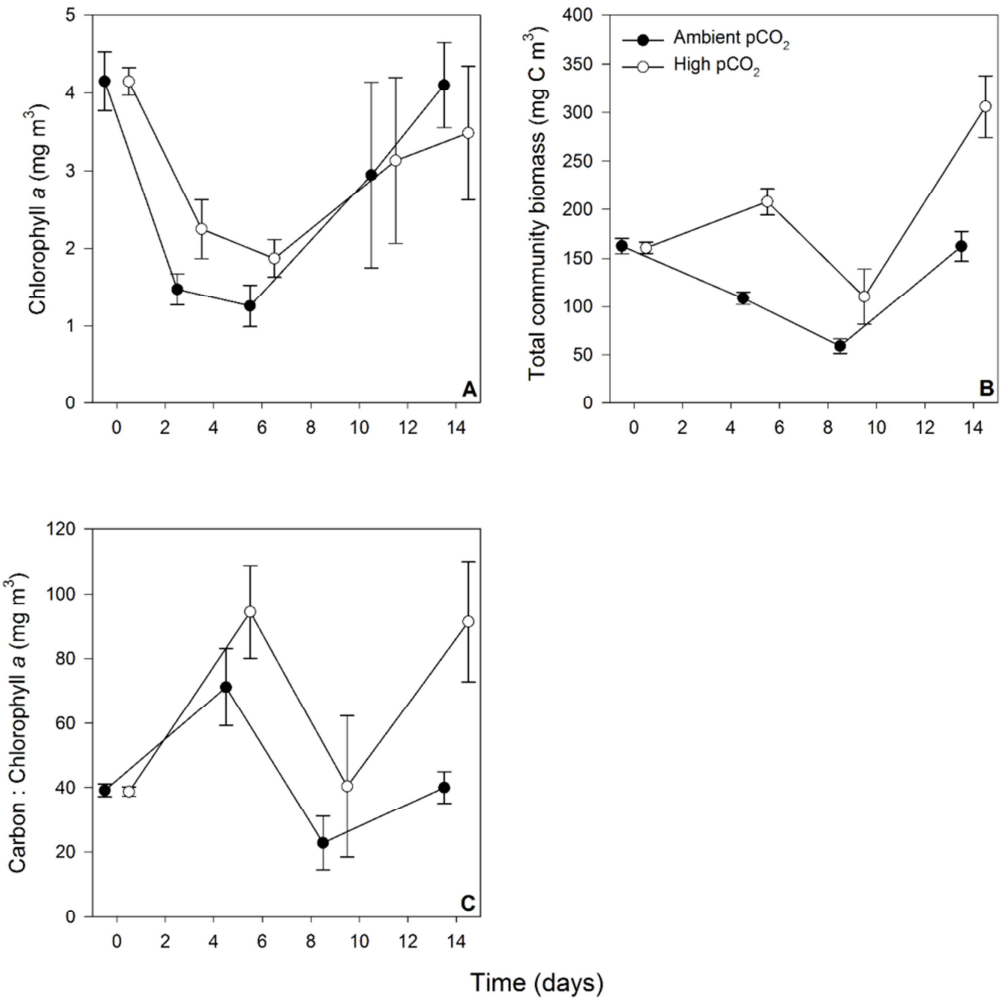

Fig 6. A. Time series of chl *a*, **B.** total phytoplankton community biomass and **C.** carbon:chl *a* ratio. Following equilibration to experimental target pCO_2 (800 µatm), no significant response to elevated pCO_2 was observed in chl *a* between the ambient control and high CO_2 treatments, however both treatments showed a significant increase in chl *a* over time. A highly significant increase in total community biomass was observed in the elevated CO_2 treatment compared to that of the ambient control. Note: time points have been displaced to display standard deviation.

its initial T0 value. In the high CO_2 treatment however, there was a significant increase in *Phaeocystis* spp. relative to the control community at T9 to T14, from 45 to 207 mg C m^3 (**Fig 7. A.**), and it dominated the community within this treatment contributing ~70% of total

community biomass, increasing by 330% compared to the T0 starting biomass (z = 3.219, p= <0.001) (**Table 2.**). Pairwise comparisons showed *Phaeocystis* spp. biomass in the high CO_2 treatment to be significantly higher than the control at T5 (t = 9.632, p < 0.001), T9 (t = 5.139, p < 0.001) and T14 (t = 10.811, p < 0.001). Between T9 and T14, colonies of *Phaeocystis spp.* were observed in both treatments in the FlowCAM images, which provided a qualitative assessment of colony presence (**Fig 7. B. & C.**).

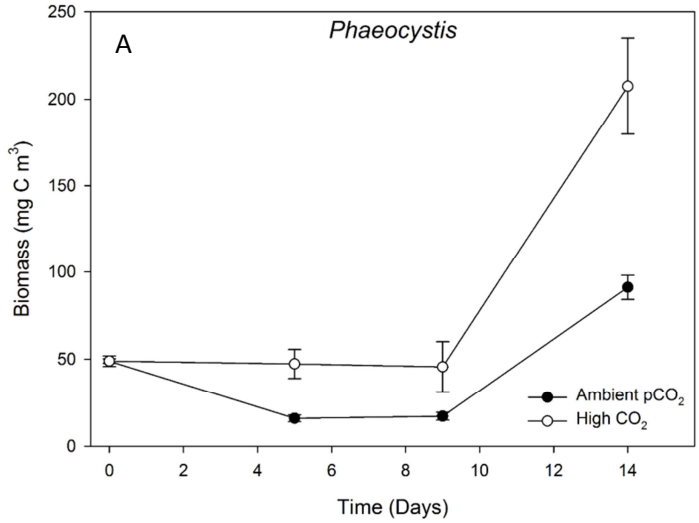

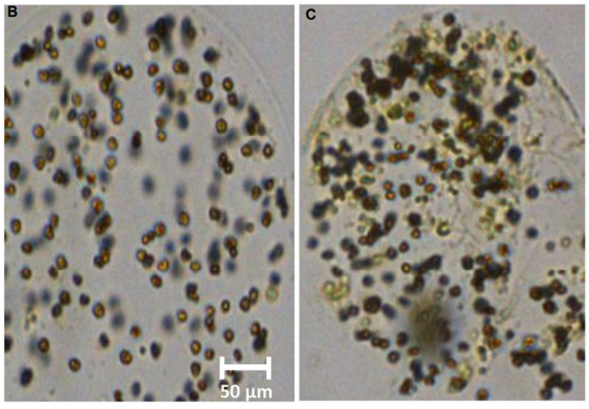

Fig 7. A. The highly significant response of *Phaeocystis* spp. to elevated pCO_2 in comparison to the ambient pCO_2 control. Note, biomass is the sum of solitary and colonial cells. **B. & C.** Image capture from FlowCAM analysis at T9 and T14 established the presence of *Phaeocystis spp.* colonies bound into a gelatinous matrix.

Nanophytoplankton biomass (excluding *Phaeocystis* spp.) declined in both treatment groups from T0 to T5, which was greater in the control community, from ~65 to 15 mg C m^3 compared to ~65 to 23 mg C m^3 in the high CO_2 treatment. Biomass increased significantly in both

treatments between T9 and T14 (z = 4.141, p = < 0.001) (**Table 2., Fig 8. A.**). Nanophytoplankton showed an overall net loss in biomass at T14 in the high CO_2 treatment (~46 mg C m^3 at T14 compared to a starting biomass of ~63 mg m^3 at T0, a decrease of 27%). A pairwise comparison however, showed nanophytoplankton biomass to be significantly greater in the high CO_2 treatment compared to the control at T14 (t = 5.297, p < 0.001).

Following an initial (acclimation) response of increased biomass between T0 and T5, picophytoplankton and *Synechococcus* both declined over time. The high CO_2 treatment maintained significantly higher biomass of picophytoplankton relative to the control following target pCO_2 equilibration (T9 to T14, t = 5.470, p < 0.001) and significantly greater biomass of *Synechococcus* which showed a net gain at T14 compared to its starting biomass value, an increase of ~60% (3.9 to 6.2 mg C m^3, **Table 2., Fig 8. D. & F.**, pairwise comparison, t = 5.239, p < 0.001). An initial short term response of increased biomass was also observed with cryptophytes in the high CO_2 treatment (T0 to T5), followed by a decrease in both control and high CO_2 treatments (T5 to T9). Between T9 and T14 however, cryptophyte biomass increased significantly in both treatments although to a greater extent in the high CO_2 treatment (pairwise comparison, t = 7.332, p < 0.001) where it was restored to the starting value of ~20 mg C m^3 compared to 9 mg C m^3 in the control (**Table 2., Fig 8. B.**).

Dinoflagellate biomass was greater in the high CO_2 treatment compared to the control at T9, however by T14 there was no significant difference between treatments (**Table 2.**). Flagellate biomass (not including *Phaeocystis* spp.) remained low and exhibited a decline in both the control and high CO_2 treatments, though the variability was high. With a mean of ~ 0.3 mg C m^3 throughout the experiment, flagellates were the lowest biomass contributor and showed no significant difference between treatments.

Ciliate biomass declined between T9 and T14 relative to the control. Both coccolithophore and diatom biomass increased between T9 and T14 in both treatments, however the increase in the high CO_2 treatment was lower compared to the control although not significantly for diatoms

(**Table 2**., **Fig 8**. **C**. & **E**.; pairwise comparisons for coccolithophores t = -3.272, p < 0.02; and diatoms t = -2.266, p < 0.276). Diatom community biomass was dominated by the chain forming *Chaetoceros curvisetus* and pennates *Proboscia alata* and *P. truncata* species. Smaller biomass

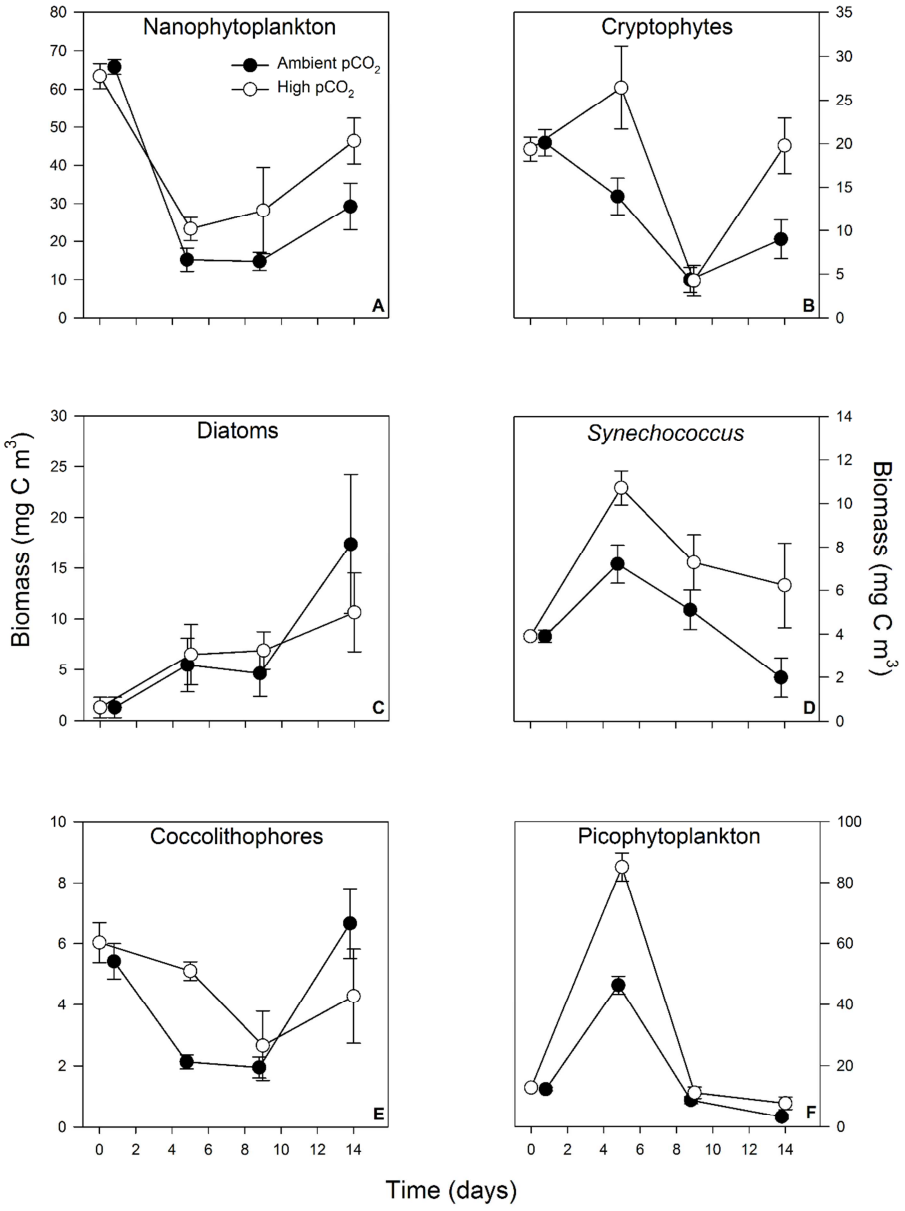

Fig 8. Response of individual components of the experimental phytoplankton community to elevated pCO_2. Cells were enumerated and converted to carbon biomass.

contributions were made by *Chaetoceros socialis, C. decipiens, C. eibenii, Leptocylindrus danicus, Pseudonitzschia spp. and Thalassiosira* spp. At T9 *Proboscia* spp. contributed 66% and 62% (~1.5 and 2.2 mg C m^3) of total diatom biomass in the control and high CO_2 treatments while *C.*

425 *curvisetus* contributed 32% and 30% (~0.5 and 0.7 mg C m^3) respectively (mean values). At T14
426 *Proboscia spp*. contributed 32% and 30% (~2.85 and 1.6 mg C m^3) of total diatom biomass
427 respectively in the control and high CO_2 treatments, while *C. curvisetus* contributed 52% and
428 34% respectively (~4.6 and 1.8 mg C m^3).

429

430 **4. Discussion**

431

432 **4.1. Trends in *Phaeocystis* spp. biomass from time-series analysis**

433 Previous analysis of the L4 phytoplankton time-series (1992-2007) elucidated distinct seasonal
434 and inter-annual changes in functional type composition as well as significant long term trends
435 in abundance. Over the study period, diatom abundance decreased while coccolithophorids, the
436 dinoflagellate *Prorocentrum cordatum* and some heterotrophic dinoflagellates and ciliates
437 increased in abundance (Widdicombe et al., 2010b). Analysis of 3 years of pCO_2 observations at
438 station L4 show an inter-annual trend of low pCO_2 in spring to high pCO_2 in autumn with a
439 concentration range of ~250 µatm to ~440 µatm (2005, 2007 and 2008). Metabolic processes
440 (i.e. photosynthesis during phytoplankton blooms), solubility and advection have been shown to
441 control seawater pCO_2 at station L4, with spring and summer showing the greatest atmospheric
442 CO_2 drawdown during stratified conditions, with CO_2 outgassing during the breakdown of
443 stratification during autumn (Litt et al., 2010).

444 Analysis of the *Phaeocystis* spp. biomass time-series at station L4 highlighted: 1) significant
445 inter-annual variability in biomass and 2) the occurrence of spring peak biomass between mid-
446 April to late May which contributed on average 17% of phytoplankton biomass between March
447 – May.

448 *Phaeocystis* spp. exhibit high temporal variability in the North Atlantic and North Sea which is
449 controlled by both meteorological and nutrient regimes (Gieskes et al., 2007).

On a global level, using 5057 observations from 1955-2009 Vogt *et al.*, (2013) showed that 64% of *Phaeocystis* spp. biomass, was recorded during spring (northern hemisphere) with more observations in the month of April compared to March and May, which we also observed in our time-series analysis. Vogt *et al.*, (2013) also showed that the minimum and maximum *Phaeocystis* spp. biomass was between 2.9 x 10^{-5} mg C m^3 and 5.4 x 10^3 mg C m^3, with a global mean of 45.7 mg C m^3 for both northern and southern hemispheres, which is similar to the mean at station L4 (41.6 mg C m^3). Inclusion of the colony mucus matrix carbon caused a significant increase in the global mean to 183.8 mg C m^3, highlighting the effect of colony mucus on the carbon budget.

In the South-eastern North Sea there was a gradual decrease in *Phaeocystis* spp. abundance from 1948 – 1970 based on Continuous Plankton Recorder survey (CPR) data (Gieskes and Kraay, 1977) . Over a 12 year period (1973 – 1985), the spring maxima in *Phaeocystis* spp. and bloom duration increased in the Marsdiep tidal inlet of the western Wadden Sea as a consequence of eutrophication (Cadée and Hegeman, 1986). In the North East Atlantic, CPR data also showed a decline in *Phaeocystis* spp. abundance from 1946 – 1987, whereas in the southern North Sea between 1980 – 1987 *Phaeocystis* spp. abundance increased (Owens et al., 1989). More recently (1988 – 2001) in the North Sea Southern Bight Belgian Coastal Zone, variations in *Phaeocystis* spp. abundance are reported to be regulated by winter nitrate enrichment supplied by riverine pulses, which are controlled by local meteorological conditions associated with the Winter North Atlantic Oscillation Index (NAO_w) (Breton et al., 2006).

4.2. Elevated pCO_2 Perturbation experiment

From the microcosm experiments we found that elevated pCO_2 to ~800 µatm caused 1) a significant increase in total community biomass by 90%, from ~160 to 305 mg C m^3, 2) significant changes in community structure from a nanophytoplankton (40%) and *Phaeocystis* spp. (30%) dominated community to a *Phaeocystis* spp. (~70%) dominated community and 3)

476 either positive or negative responses in the rest of the phytoplankton community. Both diatoms
477 and coccolithophores were the only other phytoplankton groups to show a constant increase in
478 biomass in the control treatment which was greater than that of the high CO_2 treatment, but
479 only significant for coccolithophores.

480 The overall increase in total community biomass followed the same trend as previous studies
481 conducted on natural phytoplankton community CO_2 enrichments (Feng et al., 2009; Hare et al.,
482 2007b; Riebesell et al., 2007; Tortell et al., 2008b). The only groups/species to show an overall
483 net gain in biomass in the high CO_2 treatment, irrespective of significant increases (or
484 decreases) relative to the control community following target pCO_2 equilibration were diatoms,
485 *Phaeocystis* spp. and *Synechococcus*. A number of other studies have shown that the growth
486 rates of specific diatoms can increase by 5% to 33% following 20 generations acclimated at
487 elevated pCO_2 between 750 – 1000 µatm (*Phaeodactylum tricornutum, Thalassiosira*
488 *pseudonana, T. guillardi, T. weissflogii, T. punctigera and Cocinodiscus wailesii*) (Wu et al., 2014,
489 2010) and that the highest growth occurred in diatoms > 40 µm in diameter (*T. punctigera* and
490 *C. wailesii*). Similarly in some natural phytoplankton communities exposed to elevated pCO_2
491 (750 ppmv) diatoms and prymnesiophytes become dominant, making up 60% and 30% of the
492 total biomass (Tortell *et al.*, 2002). Tortell *et al.*, (2008a) also observed in Ross Sea
493 phytoplankton, a shift in dominance from *Phaeocystis antarctica* (contributing > 90%
494 community biomass) to large chain-forming diatoms (*Chaetoceros* spp.) within high CO_2
495 treatments (800 ppmv).

496 Solitary and colonial cells of *P. globosa* exposed to high CO_2 (750 ppm) have been shown to
497 exhibit a differential response. During 14 day incubations, solitary cell biomass decreased by
498 46%, while the number of colonies increased by 26%. Maximum growth rates of colonies
499 significantly increased by 30%, but no change in growth rate was observed in solitary cells.
500 Increased particulate organic carbon (POC), nitrogen (PON) and cellular C:N ratios were also

observed under elevated CO_2 (Wang et al., 2010). This suggests that elevated CO_2 may enhance carbon export.

In a monoculture study using a *P. globosa* isolate from the South China Sea, Chen *et al*, (2014) recently showed that high CO_2 (1000 ppmv) caused a decrease in non-photochemical energy loss. Short term exposure to elevated pCO_2 in combination with low, medium and high light levels (25, 200 and 800 µmol photons m^2 s-1) resulted in reduced growth rates under high light conditions, however little effect was observed under low light conditions in short term incubations. This is in agreement with a similar study using a North Sea *P. globosa* isolate where Hoogstraten *et al*, (2012) demonstrated decreased growth rates and photosynthetic efficiency over a 6 day incubation period. However, following acclimation to experimental conditions after 9 and 14 generations, Chen *et al*, (2014) observed enhanced growth rates, increased cellular chl *a* and photosynthetic activity that had recovered to values equivalent of the control, which contradicts the findings of Hoogstraten *et al*, (2012). The authors concluded that effects of elevated CO_2 on *P. globosa* are strongly influenced not just by irradiance, but also the stage of acclimation to acidification. In our study, no decline in *Phaeocystis* spp. biomass was observed over the first 8 days under high CO_2 exposure, but biomass remained constant, followed by a significant increase to T14. Our irradiance was equal to that of the high light level applied by Chen *et al.*, (2014). This highlights the importance of distinguishing between short-term 'cellular stress' related responses and acclimated responses, as well as the time period over which experimental incubations are performed.

For *P. antarctica* in the Southern Ocean exposed to high CO_2 (current ambient, 600 and 800 ppmv), +2°C temperature increments (i.e. 2, 4 and 6°C respectively) and +50 µmol photons m^2 s^{-1} irradiance increments (i.e. 50, 100 and 150 µmol photons m^2 s^{-1}) under both Fe replete and limited conditions, there was a 64% decrease in growth rates at 800 ppmv (Fe replete) and a 46% decrease under Fe limiting conditions (Xu *et al*, 2014). The Fe replete treatment increased the percentage of solitary cells by 136% compared to 258% in the Fe limited treatment. Cellular

chl *a* decreased in the same treatments, but no influence was observed on cellular POC. The experiment also assessed the competition between *P. antarctica* and the diatom *Fragilariopsis cylindrus* and showed that the diatom dominated the population after day 8 at 800 ppmv CO_2. We did not examine the effects of macro or micro nutrients, temperature or irradiance on our *Phaeocystis* spp. community and all macro nutrients were replete. The findings of Xu *et al.*, (2014) contrast what we observed and probably reflect differences between monoclonal and two-species competition incubations and our experiment on a natural phytoplankton community. Macro nutrients in our study were equal to maximal *in situ* values (L4 mean winter values - 8μM nitrate+nitrite and 0.5 μM phosphate) providing favourable growth conditions for *Phaeocystis* spp. in both the control and elevated CO_2 treatments.

Monoclonal incubations of *Phaeocystis* spp. under different CO_2 treatments can produce variable responses related to species, strain or ecotype as well as due to differences in experimental approaches. Incubations of a natural Arctic phytoplankton community under four pH treatments (pH 8.0, 7.7, 7.4 and 7.1) showed that growth rates of *P. pouchetii* were unaffected by pH from 8.0 – 7.4. There was however, a 50% decrease in growth rates at pH 7.1 (Thoisen et al., 2015).

Accurate identification of *Phaeocystis* spp. relies on composite independent investigations combining light microscopy, transmission and scanning electron microscopy as well as flow cytometry for a complete identification of the morphotype (Rousseau et al., 2007). Such an investigation was beyond the scope and resources available for this study. Therefore, on the basis of the FlowCam image capture, current knowledge of global geographical distributions of the different *Phaeocystis* species (Verity et al., 2007) and records from station L4 phytoplankton community time-series (Widdicombe *et al.*, 2010), it is likely the *Phaeocystis* species observed in the microcosm exp. were a combination of *P. globosa* and *P. pouchetii*. The FlowCam image capture was not used to enumerate *Phaeocystis* spp. colonies since the samples were preserved with lugol's iodine which is known to cause colony disaggregation (Rutten et al.,

553 2005) which can cause an underestimation in group biomass. Flow cytometric analysis causes
554 cleavage of cell aggregations through the sheer force of sheath fluid (Dubelaar and van der
555 Reijden, 1995), and thus provides more accurate enumeration of single cells disaggregated from
556 colonies. This technique however, does not enable us to distinguish between colonial
557 cells/colonies and free living solitary cells.

558 In our experiment, the biomass range of *Phaeocystis* spp. in the control was within the range
559 measured throughout the L4 time series (~48 - 91 mg C m^3 compared to in situ values of
560 between 33 – 137 mg C m^3). The response of *Phaeocystis* spp. to the high CO_2 treatment
561 (increase of 330% from initial starting value to ~207 mg C m^3) is above the maxima measured
562 at L4. Schoemann *et al.*, (2005) illustrated the difficulties in estimating *Phaeocystis* spp. biomass
563 due to the high carbon content of the polysaccharide matrix. The difference in carbon content
564 between a solitary (without the mucus matrix carbon contribution) and colonial cell has been
565 estimated to be 42.85 – 107.85 pg C $cell^{-1}$ based on empirical methods (Jahnke and Baumann,
566 1987). Since we fixed samples in Lugol's iodine, the C biomass could be underestimated. The
567 steady state incubation conditions in our exp., (irradiance, nutrients, temperature, dilution and
568 mixing regime) may have preferentially selected for *Phaeocystis* spp. compared to the
569 fluctuating conditions of the natural environment. Sommer, (1985) demonstrated that
570 variability in resource supply controls the number and relative proportion of coexisting species
571 and using monoclonal cultures subjected to carbonate system manipulation can result in
572 significantly different growth rates of the same species (e.g. Shi *et al.*, 2009).

573

574 **4.3. Implications**

575 Dense blooms of *Phaeocystis* spp. in some ecosystems can be responsible for fish and shell-fish
576 mortality and alteration of fish taste (Levasseur et al, 1994; Peperzak & Poelman, 2008).
577 *Phaeocystis* spp. colony mucous matrix can inhibit copepod grazing, and therefore affect food
578 web structure through predator-prey size mis-match (Nejstgaard et al., 2007). Several studies

579 have found consumption rates of *Phaeocystis* spp. by copepods to be significantly lower than
580 consumption of co-occurring diatoms and heterotrophic protists during *Phaeocystis* spp.
581 blooms, showing preferential feeding strategies towards more palatable and nutritious prey
582 sources (e.g. Gasparini *et al.*, 2000; Rousseau *et al.*, 2000; Verity, 2000). Additionally,
583 carbohydrates excreted by *Phaeocystis* spp. that coagulate to form transparent exopolymer
584 particles (TEP) have strong inhibitory feeding effects on both nauplii and adult copepods (Dutz
585 et al., 2005). *Phaeocystis* spp. can also be inadequate as a food source for some copepods (e.g.
586 *Calanus helgolandicus*, *Temora stylifera* and *Acartia tonsa*), which can lead to negative effects on
587 fecundity and egg production (Tang et al., 2001; Turner et al., 2002). Stabell *et al.*, (1999)
588 extracted toxins from both *P. pouchetii* in culture and seawater samples collected during a
589 *Phaeocystis* spp. bloom, which have anaesthetic properties and can be toxic to fish larvae.
590 Exotoxins produced by *Phaeocystis* spp. during the spring bloom in the northern Norwegian
591 coast can also induce stress in cod larvae (*Gadus morhua*) (Eilertsen and Raa, 1995). Mass fish
592 mortalities have been linked to *Phaeocystis* spp. blooms in the Irish Sea (Rogers and Lockwood,
593 2009) and south-eastern Vietnamese coastal waters (Tang et al., 2004). The mass transport and
594 sedimentation of a *P. globosa* bloom in 2001 in the Oosterschelde estuary (North Sea) caused
595 anoxic conditions that led to the mass mortality of 10 million kg of *Mytilus edulis* with a market
596 value of 15 to 20 million euro (Peperzak and Poelman, 2008). *Phaeocystis* spp. are also known
597 to produce and release the cytotoxic α, β, γ, δ-unsaturated aldehyde 2-trans-4-decadienal (DD),
598 which can inhibit mitotic cell divisions. An increase in DD concentration can have a negative
599 effect on the growth rates of the diatoms *Skeletonema costatum*, *Chaetoceros socialis* and
600 *Thalassiosira antarctica* (Hansen and Eilertsen, 2007). In addition, the odorous foam produced
601 by *Phaeocystis* spp. blooms can wash up on beaches and create anoxic conditions in the surface
602 sediment which can lead to mortality of the intertidal benthic community (Desroy and Denis,
603 2004; Spilmont et al., 2009). These foam deposits also have a deleterious effect on coastal
604 tourism (Lancelot and Mathot, 1987). Our microcosm experiments suggest that future high CO_2

scenarios could increase *Phaeocystis* spp. blooms at station L4 in the WEC which could adversely affect ecosystem functioning, food web structure, fisheries and tourism.

5. Conclusion

Microcosm experiments showed that *Phaeocystis* spp. carbon biomass increased by 330% at elevated pCO_2 (~800 µatm) over a 15-day period. This study suggests that future high pCO_2 concentrations in the WEC may favour the dominance of *Phaeocystis* spp. biomass during the spring bloom, with associated negative impacts on ecosystem function and food web structure.

Acknowledgements

G.H.T and C.E.W were supported by the UK Natural Environment Research Council's (NERC) National Capability Programme – The Western English Channel Observatory (WCO) under Oceans 2025. C.E.W was also partly funded by the NERC and Department for Environment, Food and Rural Affairs, Marine Ecosystems Research Program (Grant no. NE/L003279/1). M.K. was supported by a NERC PhD studentship (grant No. NE/L50189X/1).

Table 1. Results of generalized linear models testing for the effects of pCO_2 and time on measured phytoplankton community parameters. Significance results are given as: $*$ $p < 0.05$ and $***$ $P < 0.0001$.

Response variable	n	df	*z*-value	p	sig
Chl *a* (mg m^3)					
pCO_2	32	29	1.032	0.52061	
Time	32	29	2.437	< 0.05	*
Carbon:Chl *a* (mg m^3)					
pCO_2	32	29	6.778	<0.0001	***
Time	32	29	6.684	<0.0001	***
Total community biomass (mg C m^3)					
pCO_2	32	29	12.890	<0.0001	***
Time	32	29	20.48	<0.0001	***

Table 2. Results of generalized linear models testing for the effects of pCO_2 and time on

individual phytoplankton species biomass, (n = 32). Significance results are given as: ∗ p < 0.05, and ∗∗∗ P < 0.0001.

Response variable	Parameter	df	z-value	p	sig
Ciliate biomass (mg C m^3)	pCO_2	29	2.532	0.17	
	Time	29	0.622	0.539	
Coccolithophore biomass (mg C m^3)	pCO_2	29	-1.723	0.095	
	Time	29	5.763	<0.0001	***
Cryptophyte biomass (mg C m^3)	pCO_2	29	-2.060	0.039	*
	Time	29	3.513	<0.0001	***
Diatom biomass (mg C m^3)	pCO_2	29	-1.068	0.286	
	Time	29	5.648	<0.001	***
Dinoflagellate biomass (mg C m^3)	pCO_2	29	1.567	0.117	
	Time	29	1.205	0.228	
Flagellate biomass (mg C m^3)	pCO_2	29	-0.342	0.732	
	Time	29	0.345	0.73	
Nanophytoplankton biomass (mg C m^3)	pCO_2	29	2.36	0.018	*
	Time	29	3.697	<0.0001	***
Phaeocystis biomass (mg C m^3)	pCO_2	29	3.707	<0.0001	***
	Time	29	15.636	<0.0001	***
Picophytoplankton biomass (mg C m^3)	pCO_2	29	-1.448	0.148	
	Time	29	-4.331	<0.0001	***
Synechococcus biomass (mg C m^3)	pCO_2	29	-2.334	0.027	*
	Time	29	-5.407	<0.0001	***

627

628

Table 3. Inter-annual differences in *Phaeocystis* spp. carbon biomass at station L4 between 1993 – 2014 tested with a generalised linear model. Significance results are given as: $*$ p < 0.05, $**$ p < 0.01 and $***$ p < 0.001 (n = 21).

Response variable (Year)	df	z value	p	sig
1993	20	1.458	0.144737	
1994	20	2.055	0.039883	*
1996	20	2.1	0.035769	*
1997	20	2.567	0.010258	*
1998	20	2.343	0.01915	*
1999	20	2.522	0.011669	*
2000	20	-1.009	0.313129	
2001	20	3.355	0.000794	***
2002	20	2.473	0.013411	*
2003	20	1.153	0.249038	
2004	20	2.649	0.008075	**
2005	20	-1.48	0.138741	
2006	20	-0.806	0.420182	
2007	20	1.764	0.077781	
2008	20	-0.847	0.39682	
2009	20	-0.86	0.389549	
2010	20	1.74	0.081802	
2011	20	-2.298	0.021548	*
2012	20	0.2	0.841177	
2013	20	2.34	0.019302	*
2014	20	2.405	0.016167	*

References

Alley, D., Berntsen T, Bindoff NL, Chen ZL, Chidthaisong A, Friedlingstein P, Gregory J G, Hegerl Heimann M, Hewitson B, Hoskins B, Joos F, Jouzel, Kattsov V, Lohmann U, Manning M, Matsuno T, Molina M, Nicholls N, Verpeck J, Qin DH, Raga G, Ramaswamy V, Ren JW, Rusticucci M, Solomon S, Somerville R, Stocker TF, Stott P, Stouffer RJ, Whetton P, Wood RA and Wratt D. (2007). *Climate Change 2007*. The Physical Science basis: Summary for

638 policymakers. Contribution of Working Group I to the Fourth Assessment Report of the
639 Intergovernmental Panel on Climate Change.
640
641 Barcelos e Ramos J, Müller MN, Riebesell U. (2010). Short-term response of the coccolithophore
642 *Emiliania huxleyi* to an abrupt change in seawater carbon dioxide concentrations.
643 *Biogeosciences*, **7**, 177–186.
644 Booth BC. (1988). Size classes and major taxonomic groups of phytoplankton at two locations in
645 the subarctic Pacific Ocean in May and August, 1984. *Marine Biology*, **97**, 275–286.
646 Boyd PW, Doney SC. (2002). Modelling regional responses by marine pelagic ecosystems to
647 global climate change. *Geophysical Research Letters*, **29**, 1–4.
648 Breton E, Parent J, Lancelot C, Rousseau V, Ozer J. (2006). Hydroclimatic modulation of diatom /
649 *Phaeocystis* blooms in nutrient-enriched Belgian coastal waters (North Sea). *Limnology and*
650 *Oceanography*, **51**, 1401–1409.
651 BS EN 15204 (2006). Water quality – Guidance standard on the enumeration of phytoplankton
652 using inverted microscopy (Utermöhl technique). British Standards Institution.
653 Burkhardt S, Riebesell R. (1997). CO_2 availability affects elemental composition (C:N:P) of the
654 marine diatom Skeletonema costatum. *Marine Biotechnology*, 155, 67-76.
655 Cadée GC, Hegeman J. (1986). Seasonal and annual variation in *Phaeocystis pouchetii*
656 (haptophyceae) in the westernmost inlet of the Wadden Sea during the 1973 to 1985
657 period. *Netherlands Journal of Sea Research*, **20**, 29–36.
658 Cadée GC, Hegeman J. (2002). Phytoplankton in the Marsdiep at the end of the 20th century; 30
659 years monitoring biomass, primary production, and *Phaeocystis* blooms. *Journal of Sea*
660 *Research*, **48**, 97–110.
661 Chen S, Gao K. (2011). Solar ultraviolet radiation and CO_2-induced ocean acidification interacts
662 to influence the photosynthetic performance of the red tide alga *Phaeocystis globosa*

(Prymnesiophyceae). *Hydrobiologia*, **675**, 105–117.

Chen S, Beardall J, Gao K. (2014). A red tide alga grown under ocean acidification upregulates its tolerance to lower pH by increasing its photophysiological functions. *Biogeosciences*, **11**, 4829–4837.

Coello-Camba A, Agusti S, Holding J, Arrieta J A, and Duarte C M. (2014). Interactive effect of temperature and CO2 increase in Arctic phytoplankton. *Frontiers in Marine Science*, 1, 1-10.

Desroy N, Denis L. (2004). Influence of spring phytodetritus sedimentation on intertidal macrozoobenthos in the eastern English Channel. *Marine Ecology Progress Series*, **270**, 41–53.

Dickson AG, Millero FJ. (1987). A comparison of the equilibrium constants for the dissociation of carbonic acid in seawater media. *Deep Sea Research Part I: Oceanographic Research Papers*, **34**, 1733–1743.

DiTullio GR, Grebmeier JM, Arrigo KR, Lizotte, M P, Robinson, D H, Leventer, A, Barry, J P, VanWoert, M L, Dunbar, R B. (2000). Rapid and early export of *Phaeocystis antarctica* blooms in the Ross Sea, Antarctica. *Nature*, **404**, 595–598.

Doney SC, Fabry VJ, Feely R A., Kleypas J A. (2009). Ocean Acidification: The Other CO_2 Problem. *Annual Review of Marine Science*, **1**, 169–192.

Dubelaar GBJ, van der Reijden CS. (1995). Size distributions of *Microcystis aeruginosa* colonies: a flow cytometric approach. *Water Science and Technology*, **32**, 171–176.

Dutz J, Klein Breteler WCM, Kramer G. (2005). Inhibition of copepod feeding by exudates and transparent exopolymer particles (TEP) derived from a *Phaeocystis globosa* dominated phytoplankton community. *Harmful Algae*, **4**, 929–940.

Eilertsen H, Raa J. (1995). Toxins in seawater produced by a common phytoplankter : *Phaeocystis pouchetii*. *Journal of marine biotechnology*, **3**, 115–119.

687 Eilertsen HC, Taasen JP, WesIawski JM. (1989). Phytoplankton studies in the fjords of West
688 Spitzbergen: physical environment and production in spring and summer. *Journal of*
689 *Plankton Research* , **11** , 1245–1260.

690 Endo H, Yoshimura T, Kataoka T, Suzuki K. (2013). Effects of CO_2 and iron availability on
691 phytoplankton and eubacterial community compositions in the northwest subarctic
692 Pacific. *Journal of Experimental Marine Biology and Ecology*, **439**, 160–175.

693 Feng Y, Warner ME, Zhang Y, Sun J, Fu F-X, Rose JM, Hutchins D A. (2008). Interactive effects of
694 increased pCO_2, temperature and irradiance on the marine coccolithophore *Emiliania*
695 *huxleyi* (Prymnesiophyceae). *European Journal of Phycology*, **43**, 87–98.

696 Feng Y, Hare C, Leblanc K, Rose JM, Zhang Y, DiTullio GR, Lee PA, Wilhelm SW, Rowe JM, Sun J,
697 Nemcek N, Gueguen C, Passow U, Benner I, Brown C, Hutchins DA. (2009). Effects of
698 increased pCO_2 and temperature on the North Atlantic spring bloom. I. The phytoplankton
699 community and biogeochemical response. *Marine Ecology Progress Series*, **388**, 13–25.

700 Feng Y, Hare C E, Rose J M, Handy S M, DiTullio G R, Lee P A, Smith W O, Peloquin J, Tozzi S. Sun J,
701 Zhang Y, Dunbar R B, Long MC, Sohst B, Lohan M and Hutchins D A. (2010). Interactive
702 effects of iron, irradiance and CO_2 on Ross Sea Phytoplankton. *Deep Sea Research Part I*, 57,
703 3, 368-383.

704 Gao K, Campbell DA. (2014). Photophysiological responses of marine diatoms to elevated CO_2
705 and decreased pH: A review. *Functional Plant Biology*, **41**, 449–459.

706 Gasparini S, Daro MH, Antajan E, Tackx M, Rousseau V, Parent JY, Lancelot C. (2000).
707 Mesozooplankton grazing during the *Phaeocystis globosa* bloom in the southern bight of
708 the North Sea. *Journal of Sea Research*, **43**, 345–356.

709 Gieskes WWC, Kraay GW. (1977). Continuous plankton records: Changes in the plankton of the
710 North Sea and its eutrophic southern bight from 1948 to 1975. *Netherlands Journal of Sea*
711 *Research*, **11**, 334–364.

712 Gieskes WWC, Leterme SC, Peletier H, Edwards M, Reid PC. (2007). *Phaeocystis* colony
713 distribution in the North Atlantic Ocean since 1948, and interpretation of long-term
714 changes in the *Phaeocystis* hotspot in the North Sea. *Biogeosciences*, **83**, 49–60.

715 Hansen E, Eilertsen HC. (2007). Do the polyunsaturated aldehydes produced by *Phaeocystis*
716 *pouchetii* (Hariot) Lagerheim influence diatom growth during the spring bloom in
717 Northern Norway? *Journal of Plankton Research*, **29** , 87–96.

718 Hare C, Leblanc K, DiTullio G, Kudela RM, Zhang Y, Lee PA, Riseman S, Hutchins DA. (2007).
719 Consequences of increased temperature and CO_2 for phytoplankton community structure
720 in the Bering Sea. *Marine Ecology Progress Series*, **352**, 9–16.

721 Harris R (2010). The L4 time-series: the first 20 years. *Journal of Plankton Research*, **32**, 577–
722 583.

723 Herberich E, Sikorski J, Hothorn T. (2010). A Robust Procedure for comparing multiple means
724 under heteroscedasticity in unbalanced designs. *PLoS ONE*, **5**,
725 http://dx.doi.org/10.1371/journal.pone.0009788

726 Hoogstraten A., Peters M, Timmermans KR, De Baar HJW. (2012). Combined effects of inorganic
727 carbon and light on *Phaeocystis globosa* Scherffel (Prymnesiophyceae). *Biogeosciences*, **9**,
728 1885–1896.

729 Jahnke J, Baumann MEM. (1987). Differentiation between *Phaeocystis pouchetii* (Har.)
730 Lagerheim and *Phaeocystis globosa* Scherffel. *Hydrobiological Bulletin*, **21**, 141–147.

731 Kim J M, Lee K, Shin K, Kang J H, Lee H W, Kim M, Jang P G, and Jang M C. (2006). The effect of
732 seawater CO_2 on growth of a natural phytoplankton assemblage in a controlled mesocosm
733 experiment. *Limnology and Oceanography*, 51, 4, 1629-1636.

734 Kovala PE, Larrance JD. (1966). *Computation of phytoplankton cell numbers, cell volume, cell*
735 *surface and plasma volume per liter from microscopical counts.* DTIC Document.

736 Lancelot C, Mathot S. (1987). Dynamics of a *Phaeocystis*-dominated spring bloom in Belgian

737 coastal waters. I. Phytoplanktonic activities and related parameters. *Marine Ecology*
738 *Progress Series*, **37**, 249–257.

739 Lancelot C, Rousseau V, Schoemann V. and Becquevort, S. (2002). On the ecological role of the
740 different life forms of *Phaeocystis*. *Proceedings of the EC workshop LIFEHAB: Life histories of*
741 *microalgal species causing harmful blooms*, 214.

742 Lancelot C, Rousseau V, Gypens N. (2009). Ecologically based indicators for *Phaeocystis*
743 disturbance in eutrophied Belgian coastal waters (Southern North Sea) based on field
744 observations and ecological modelling. *Journal of Sea Research*, **61**, 44–49.

745 Liss P, Malin G, Turner S, Holligan P. (1994). Dimethyl sulphide and *Phaeocystis*: A review.
746 *Journal of Marine Systems*, **5,** 41-53.

747 Litt E J, Hardman-Mountford N J, Blackford J C, Mitchelson-Jacob G, Goodman A, Moore G F,
748 Cummings D G, and Butenschon M. (2010). Biological control of pCO_2 at station L4 in the
749 Western English Channel over 3 years. *Journal of Plankton Research*, 32, 5, 621-629.

750 Love BA, Olson MB, Wuori T. (2016). Technical Note: A minimally-invasive experimental system
751 for pCO_2 manipulation in plankton cultures using passive gas exchange (Atmospheric
752 Carbon Control Simulator). *Biogeosciences Discussions*, 1–19.

753 Mehrbach C, Culberson CH, Hawley JE, Pytkowicz RM. (1973). Measurement of the Apparent
754 Dissociation Constants of Carbonic Acid in Seawater at Atmospheric Pressure. *Limnology*
755 *and Oceanography*, **18**, 897–907.

756 Menden-Deuer S, Lessard EJ. (2000). Carbon to volume relationships for dinoflagellates,
757 diatoms, and other protist plankton. *Limnology and Oceanography*, **45**, 569–579.

758 Muller-Karger FE. (2005). The importance of continental margins in the global carbon cycle.
759 *Geophysical Research Letters*, **32**, L01602.

760 Nejstgaard JC, Tang KW, Steinke M, Dutz J, Koski M, Antajan E, Long JD. (2007). Zooplankton
761 grazing on *Phaeocystis*: A quantitative review and future challenges. *Biogeochemistry*, **83**,

762 147–172.

763 Orr JC, Bopp L J, Fabry VJ, Aumont O, Doney SC, Feely RA, Gnanadesikan A, Gruber N, Ishida A,
764 Joos F, Key RM, Lindsay K, Maier-Reimer E, Matear R, Monfray P, Mouchet A, Najjar RG,
765 Plattner GK, Rodgers KB, Sabine CL, Sarmiento JL, Schlitzer R, Slater RD, Totterdell IJ,
766 Weirig MF, Yamanaka Y, and Yool A. (2005). Anthropogenic ocean acidification over the
767 twenty-first century and its impact on calcifying organisms. *Nature*, **437**, 681–6.

768 Ospar S, Report I. (2009). Eutrophication Status of the OSPAR Maritime Area Second OSPAR
769 Integrated Report Eutrophication Series.

770 Owens NJP, Cook D, Colebrook M, Hunt H, Reid PC. (1989). Long Term Trends in the Occurrence
771 of *Phaeocystis* Sp. in the North-East Atlantic. *Journal of the Marine Biological Association of*
772 *the United Kingdom*, **69**, 813.

773 Peperzak L, Poelman M. (2008). Mass mussel mortality in The Netherlands after a bloom of
774 *Phaeocystis globosa* (prymnesiophyceae). *Journal of Sea Research*, **60**, 220–222.

775 Pierrot D, Lewis E, Wallace DWR (2006). MS Excel program developed for CO_2 system
776 calculations. *ORNL/CDIAC-105a. Carbon Dioxide Information Analysis Center, Oak Ridge*
777 *National Laboratory, US Department of Energy, Oak Ridge, Tennessee*.

778 Poulton NJ, Martin JL. (2010). Imaging flow cytometry for quantitative phytoplankton analysis -
779 FlowCAM. *Microscopic and molecular methods for quantitative phytoplankton analysis*, 47–
780 54.

781 Raupach MR, Marland G, Ciais P, Le Quéré C, Canadell JG, Klepper G, Field CB. (2007). Global and
782 regional drivers of accelerating CO_2 emissions. *Proceedings of the National Academy of*
783 *Sciences of the United States of America*, **104**, 10288–93.

784 Raven. J., Caldeira. K., Elderfield. H. H-G and others. (2005). Ocean acidification due to increasing
785 atmospheric carbon dioxide. *The Royal Society*.

786 Riebesell, U. (2004). Effects of CO_2 Enrichment on Marine Phytoplankton. J. Oceanogr. **60**, 719–

729. doi:10.1007/s10872-004-5764-z

Riebesell U, Schulz KG, Bellerby RGJ, Botros M, Fritsche P, Meyerhöfer M, Neill C, Nondal G, Oschlies A, Wohlers J, Zöllner, E. (2007). Enhanced biological carbon consumption in a high CO_2 ocean. *Nature*, **450**, 545–8.

Riebesell U, Fabry VJ, Hansson L, Gattuso J-P. (2010). *Guide to best practices for ocean acidification* (ed U. Riebesell, V. J. Fabry LH and J –P. GL). Publications Office of The European Union.

Rogers SI, Lockwood SJ. (2009). Observations on coastal fish fauna during a spring bloom of *Phaeocystis pouchetii* in the eastern Irish Sea. *Journal of the Marine Biological Association of the United Kingdom*, **70**, 249-253.

Rousseau V, Becquevort S, Parent J, Gasparini S, Daro M, Tackx M, Lancelot C. (2000). Trophic efficiency of the planktonic food web in a coastal ecosystem dominated by *Phaeocystis* colonies. *Journal of Sea Research*, **43**, 357–372.

Rousseau V, Chrétiennot-Dinet M-J, Jacobsen A, Verity P, Whipple S. (2007). The life cycle of *Phaeocystis*: state of knowledge and presumptive role in ecology. *Biogeochemistry*, **83**, 29–47.

Rutten TP, Sandee B, Hofman ART. (2005). Phytoplankton monitoring by high performance flow cytometry: A successful approach? *Cytometry Part A*, **64**, 16–26.

Schoemann V, Becquevort S, Stefels J, Rousseau V, Lancelot C. (2005). *Phaeocystis* blooms in the global ocean and their controlling mechanisms: a review. *Journal of Sea Research*, **53**, 43–66.

Schulz KG, Riebesell U, Bellerby RGJ, Biswas H, Meyerhöfer M, Müller M N, Egge J K, Nejstgaard J C, Neill C, Wohlers J, Zöllner E. (2008). Build-up and decline of organic matter during PeECE III. *Biogeosciences*, **5**, 707–718.

Schulz KG, Ramos JB, Zeebe RE, Riebesell U. (2009). Biogeosciences CO_2 perturbation

812 experiments: similarities and differences between dissolved inorganic carbon and total
813 alkalinity manipulations. *Biogeosciences*, **6**, 2145–2153.

814 Shi D, Xu Y, Morel FMM. (2009). Effects of the pH/pCO_2 control method on medium chemistry
815 and phytoplankton growth. *Biogeosciences*, **6**, 1199–1207.

816 Smyth TJ, Fishwick JR, AL-Moosawi L, Cummings DG, Harris C, Kitidis v, Rees A, Martinez-
817 Vicente V and Woodward EMS. (2010). A broad spatio-temporal view of the Western
818 English Channel observatory. *Journal of Plankton Research*, **32**, 585–601.

819 Sommer U. (1985). Comparison between steady state and non-steady state competition:
820 Experiments with natural phytoplankton. *Limnology and Oceanography*, **30**, 335–346.

821 Spilmont N, Denis L, Artigas LF, Caloinc F, Courcotb L, Créachd A, Desroye N, Gevaerta F,
822 Hacquebarta P, Hubasb C, Janquina MA, Lemoined Y, Luczaka C, Migné A, Raucha M,
823 Davoultf D. (2009). Impact of the *Phaeocystis globosa* spring bloom on the intertidal
824 benthic compartment in the eastern English Channel: A synthesis. *Marine Pollution*
825 *Bulletin*, **58**, 55–63.

826 Stabell OB, Aanesen RT, Eilertsen HC. (1999). Toxic peculiarities of the marine alga *Phaeocystis*
827 *pouchetii* detected by in vivo and in vitro bioassay methods. *Aquatic Toxicology*, **44**, 279–
828 288.

829 Stefels J, Dijkhuizen L, Gieskes WW. (1995). DMSP-lyase activity in a spring phytoplankton
830 bloom off the Dutch coast, related to *Phaeocystis* sp. abundance. *Marine Ecology Progress*
831 *Series*, **123**, 235–244.

832 Tang KW, Jakobsen HH, Visser AW. (2001). *Phaeocystis globosa* (Prymnesiophyceae) and the
833 planktonic food web: Feeding, growth, and trophic interactions among grazers. *Limnology*
834 *and Oceanography*, **46**, 1860–1870.

835 Tang DL, Kawamura H, Hai D-N, Takahashi W. (2004). Remote sensing oceanography of a
836 harmful algal bloom off the coast of south-eastern Vietnam. *Journal of Geophysical*

Research, **109**, 1–7.

Tarran G A, Heywood JL, Zubkov M V. (2006). Latitudinal changes in the standing stocks of nano- and picoeukaryotic phytoplankton in the Atlantic Ocean. *Deep Sea Research Part II: Topical Studies in Oceanography*, **53**, 1516–1529.

Tett P, Gowen R, Mills D, Fernandes T, Gilpin L, Huxham M, Kennington K, Read P, Service M, Wilkinson M, Malcolm S. (2007). Defining and detecting undesirable disturbance in the context of marine eutrophication. *Marine pollution bulletin*, **55**, 282–97.

Thoisen C, Riisgaard K, Lundholm N, Nielsen T, Hansen P. (2015). Effect of acidification on an Arctic phytoplankton community from Disko Bay, West Greenland. *Marine Ecology Progress Series*, **520**, 21–34.

Tortell P, DiTullio G, Sigman D, Morel F. (2002). CO_2 effects on taxonomic composition and nutrient utilization in an Equatorial Pacific phytoplankton assemblage. *Marine Ecology Progress Series*, **236**, 37–43.

Tortell PD, Payne CD, Li Y, Trimborn S, Rost B, Smith W O, Riesselman C, Dunbar R, Sedwick P, DiTullio GR. (2008). CO_2 sensitivity of Southern Ocean phytoplankton. *Geophysical Research Letters*, **35**, L04605.

Turner JT, Ianora A, Esposito F, Carotenuto Y, Miralto A. (2002). Zooplankton feeding ecology: does a diet of *Phaeocystis* support good copepod grazing, survival, egg production and egg hatching success? *Journal of Plankton Research*, **24**, 1185–1195.

Utermöhl H. (1958). Zur vervollkommnung der quantitativen phytoplankton-methodik. *Mitt. int. Ver. theor. angew. Limnol.*, **9**, 1–38.

Verity PG. (2000). Grazing experiments and model simulations of the role of zooplankton in *Phaeocystis* food webs. *Journal of Sea Research*, **43**, 317–343.

Verity PG, Brussaard CP, Nejstgaard JC, Van Leeuwe M A., Lancelot C, Medlin LK. (2007). Current understanding of *Phaeocystis* ecology and biogeochemistry, and perspectives for future

862 research (eds Leeuwe MA van, Stefels J, Belviso S, Lancelot C, Verity PG, Gieskes WWC).
863 Springer Netherlands, 311-330 pp.

864 Vogt M, O'Brien C, Peloquin J, Schoemann V, Breton E, Estrada M, Gibson J, Karentz D, Van
865 Leeuwe M A, Stefels J, Widdicombe C & Peperzak L. (2012). Global marine plankton
866 functional type biomass distributions: Phaeocystis spp. *Earth System Science Data*, **4**, 107-
867 120.

868 Wang Y, Smith WO, Wang X, Li S. (2010). Subtle biological responses to increased CO_2
869 concentrations by Phaeocystis globosa Scherffel, a harmful algal bloom species. *Geophysical*
870 *Research Letters*, **37**, 1–5.

871 Wassmann P, Vernet M, Mitchell B, Rey F (1990). Mass sedimentation of *Phaeocystis pouchetii* in
872 the Barents Sea. *Marine Ecology Progress Series*, **66**, 183–195.

873 Welschmeyer. (1994). Fluorometric analysis of chlorophyll a in the presence of chlorophyll b
874 and pheopigments. *Limnology and Oceanography*, **39**, 1985–1992.

875 Widdicombe CE, Eloire D, Harbour D, Harris RP, Somerfield PJ. (2010). Long-term
876 phytoplankton community dynamics in the Western English Channel. *Journal of Plankton*
877 *Research*, **32**, 643–655.

878 Wolf-gladrow BDA, Riebesell U, Burkhardt S, Jelle B. (1999). Direct effects of CO_2 concentration
879 on growth and isotopic composition of marine plankton. *Tellus*, **51B**, 461–476.

880 Wollast R. (1998). *"Evaluation and comparison of the global carbon cycle in the coastal zone and*
881 *in the open ocean." The sea*. 213-252 pp.

882 Woodward EMS, Rees AP. (2001). Nutrient distributions in an anticyclonic eddy in the northeast
883 Atlantic Ocean, with reference to nanomolar ammonium concentrations. *Deep-Sea*
884 *Research Part II: Topical Studies in Oceanography*, **48**, 775–793.

885 Wu Y, Gao K, Riebesell U. (2010). CO_2-induced seawater acidification affects physiological
886 performance of the marine diatom *Phaeodactylum tricornutum*. *Biogeosciences*, **7**, 2915–

887 2923.

888 Wu Y, Campbell D A., Irwin AJ, Suggett DJ, Finkel Z V. (2014). Ocean acidification enhances the
889 growth rate of larger diatoms. *Limnology and Oceanography*, **59**, 1027–1034.

890 Xu K, Fu F-X, Hutchins D A. (2014). Comparative responses of two dominant Antarctic
891 phytoplankton taxa to interactions between ocean acidification, warming, irradiance, and
892 iron availability. *Limnol. Oceanog*, **59**, 1919–1931.